ANALYSIS OF THERMOACOUSTIC INSTABILITES IN A MICRO GAS TURBINE

C. Vankelekom*, F.G. Schiavone **, W. De Paepe*, D. Laera **
christophe.vankelekom@student.umons.ac.be
*University of Mons (UMONS), Thermal Engineering and Combustion Research Unit, Mons, Belgium
**Department of Mechanics, Mathematics and Management, Polytechnic University of Bari, Bari, Italy

Abstract
Global warming, environmental impact, pollution and air quality are the main concerns of this century. One way to limit the impact is to reduce our fossil fuel consumption for electricity production using renewable energy sources. This solution, however, is intermittent and non-dispatchable. To help the energy transition, thermal-based power generation as micro gas turbines (mGTs) offer many prospects, thanks to their flexible operation, such as short start-up times. Nevertheless, thermoacoustic instabilities can occur, and a way to identify, quantify and even prevent them is of fundamental importance. With this work, we aim to numerically characterize the onset of these instabilities in the MTT EnerTwin mGT fuelled with natural gas, to gain a better understanding of the mechanisms leading to flame-acoustic coupling in these devices.

Introduction
The thermoacoustic combustion instabilities is an unsteady non-linear phenomenon generated by the coupling between heat release rate fluctuations and acoustic waves. This kind of instability is dangerous because pressure fluctuations may produce vibrations inside the system that could further damage the components. Fully compressible Large Eddy Simulations (LES) have been proved to be a powerful tool to investigate this phenomenon in either laboratory scales [1] or industrial gas turbines [2]. Nevertheless, such methodology has never been applied in micro gas turbines (mGTs) with very small-scale combustor. The present work aims at filling this gap by proposing a LES study on thermoacoustic instabilities in a mGT. At first, stable flame is characterized. LES predict a fully premixed V-shape flame burning in very lean conditions. Acoustic properties of inlet and outlet boundary conditions are then varied to trigger the thermoacoustic modes. Differently from standard gas turbines, unstable modes at very high frequencies, i.e., 920 and 2260 Hz, are predicted and are in line with experimental recordings performed in the TRMI laboratory at UMONS (Belgium). The applied procedure has been proved to be relevant to analyse thermoacoustic instabilities via numerical LES simulations.

Experimental set-up

The considered burner is integrated in the MTT EnerTwin micro gas turbine, exploiting the typical recuperator Brayton cycle layout. It combines heat and power generation and produces up to 3 kWe and up to 21.5 kWth. A simplified scheme of the experimental set-up of this mGT, available in the laboratories of UMONS, with the different sensor locations where P, T and $\dot{V}$ (pressure, temperature, and volumetric flow rate, respectively) are measured, is presented in Fig. 1a. The mGT is equipped with a concentric co-flow cylindrical partially pre-mixed combustor, a scheme of which is provided in Fig. 1b. The air (blue arrows) is distributed over the primary zone, bypassing through the swirler and the secondary and tertiary zones thanks to dilution holes (denoted with the letter A). This swirler is composed of 7 blades, inducing the swirling motion of the air, and has 14 fuel injectors, placed upstream of the blades where fuel (in this study, methane) is injected (red arrows).
Finally, in nominal operation, the combustor operates at a pressure of 2.8 bar with an air mass flow rate of 45 g/s at 975 K and a methane mass flow rate of 0.43 g/s at 380 K. As a result, the global equivalence ratio is equal to 0.165. These operating conditions are used for the numerical simulation of the combustor.

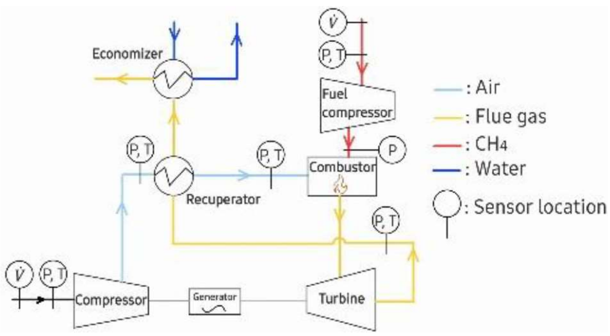

(a)

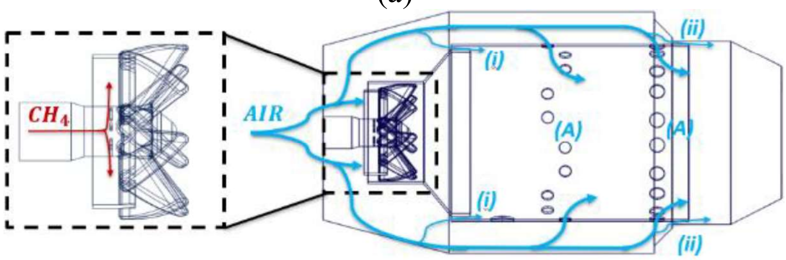

(b)

Figure 1. (a) Simplified scheme of the mGT set-up with the component links and sensor locations. (b) Combustor geometry with a local view on the swirler region where methane is injected upstream of the swirler and air is divided through several passages: swirler, dilution holes (A), inlet gap (*i*) and outlet gap (*ii*).

Numerical set-up and methodology

To investigate thermoacoustic instabilities, fully compressible Large Eddy Simulations are used to solve the reacting multi-species Navier-Stokes equation. The mesh used has 25 million tetrahedral elements and is refined in the flame region with a cell size of 0.35 mm. A smooth transition towards the outlet is achieved to reach a maximum size of 3 mm. These simulations are performed with the AVBP code developed at CERFACS (https://www.cerfacs.fr/avbp7x/). Firstly, to characterize the stable flame, thermoacoustic coupling is prevented imposing a non-reflective outlet via Navier-Stokes Characteristic Boundary Conditions (NSCBC) [3]. Walls are considered as no-slip and with heat losses for the ones closer to the flame region. The flux through the wall is evaluated by giving the thermal resistance, equal to $2.5 \cdot 10^{-5}$ m²K/W, computed as the ratio of the wall thickness and the heat conductivity. For the combustion model, a dynamic version of the thickened flame model (DTFLES) is applied [4] coupled with the Charlette efficiency function [5, 6] with $\beta = 0.5$. To model the small turbulence scales, the SIGMA model is used as subgrid stress tensor [7]. Pure methane is considered as fuel and its oxidation is described with a modified version of the two-step BFER mechanism [9] (more details are reported in the next section). Once the reactive flow is converged, the results are used to compute the acoustic modes with FEniCS (https://fenicsproject.org/), a code solving the Helmholtz equation with a Finite Element Method. Finally, the thermoacoustic analysis is carried out by varying the relaxation factor at the inlet and outlet (NSCBC) to trigger thermo-acoustic instability [9].

Chemical mechanism for partially pre-mixed flame

The used chemical mechanism consists of two chemical reactions (1) and (2). To correctly predict the velocity and thickness of the flame for the operating condition in this work, an optimization is performed by changing the coefficients of the Arrhenius reaction rate constant equations (Eqs. (1) and (2)) and the Pre-Exponential Adjustment (PEA) functions (Eqs. (3) and (4)):

$$CH_4 + 1.5\, O_2 \Rightarrow CO + 2\, H_2O \qquad k_1 = A_1\, f_1(\phi)\, T^{\beta_1}\, e^{\left(\frac{-E_{a1}}{RT}\right)} [CH_4]^{n_{CH_4}}\, [O_2]^{n_{O_{2,1}}} \quad (1)$$

$$CO + 0.5\, O_2 \Leftrightarrow CO_2 \qquad k_2 = A_2\, f_2(\phi)\, T^{\beta_2}\, e^{\left(\frac{-E_{a2}}{RT}\right)} [CO]^{n_{CO}}\, [O_2]^{n_{O_{2,2}}} \quad (2)$$

$$f_1(\phi) = \frac{2}{1+\tanh\left(\frac{\phi_{0,1}-\phi}{\sigma_{0,1}}\right) + B_1\left[1+\tanh\left(\frac{\phi-\phi_{1,1}}{\sigma_{1,1}}\right)\right] + C_1\left[1+\tanh\left(\frac{\phi-\phi_{2,1}}{\sigma_{2,1}}\right)\right]} \quad (3)$$

$$f_2(\phi) = \frac{1}{2}\left[1+\tanh\left(\frac{\phi_{0,2}-\phi}{\sigma_{0,2}}\right)\right] + \frac{B_2}{2}\left[1+\tanh\left(\frac{\phi-\phi_{1,2}}{\sigma_{1,2}}\right)\right] + \frac{C_2}{2}\left[1+\tanh\left(\frac{\phi-\phi_{2,2}}{\sigma_{2,2}}\right)\right]\left[1+\tanh\left(\frac{\phi_{3,2}-\phi}{\sigma_{3,2}}\right)\right] \quad (4)$$

The optimization was performed to minimize the root mean square of the velocity difference predicted by the BFER and GRI 3.0 detailed mechanisms computed by using Cantera (https://cantera.org/). The optimized values (reported in red) of the novel *"CH4_6_2_CV"* mechanism are summarized in Table 1 where standard BFER parameters are also reported (in black). For the PEA functions, only the parameters $\phi_{2,1}$ has been modified from a value of 1.6 to 1.68. The Prandtl and the Schmidt numbers for each species are imposed as equal to 0.5, keeping a constant Lewis number equal to 1. Figure 2 shows the improvement with the new mechanism (blue curve), with respect to the classic BFER (black curve) especially for lean mixtures.

Table 1. Parameters of the Arrhenius reactions rate constant equations for the CH4_6_2_CV (red) and standard BFER (black) schemes.

j	A_j	β_j	$E_{a,j}$	$n_{O_{2,j}}$	n_{CH_4}	n_{CO}
1	4.9×10^9 8.21×10^7	0	3.55×10^4 4.41×10^4	0.65 0.542	0.5 0.2	/
2	2×10^8 1×10^8	0.7	1.2×10^4	0.5	/	1

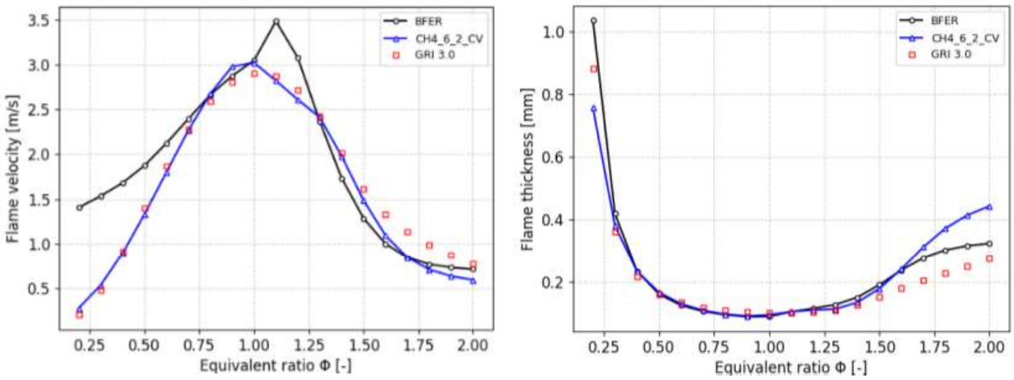

(a) (b)

Figure 2. Comparison of the 1D flame velocity (a) and thickness (b) between the GRI 3.0, BFER and the new CH4_6_2_CV mechanisms.

Reactive flow results: stable flame

Figure 3a depicts an instantaneous 3D contour of the heat release rate coloured by the DTFLES thickening factor and local equivalence ratio: LES predicts a classical V-shape flame stabilized over the swirler nose. Figure 3b reports a scatter plot of temperature over local equivalence ratio. The flame mainly burns in lean regime with the most probable value around ϕ=0.55, confirming the need of using the improved CH4_6_2_CV mechanism.

Then, the time averaged of the temperature field over 5 flow-through times is reported in Fig. 4. It provides a better visualization of the flame detachment from injector walls, shown by the white iso-contour of heat release rate at 10% of the maximum value, as a consequence of heat losses.

Thermoacoustic studies

By analysing the spectrum of pressure probes located at the inlet of the combustor (Fig. 5a-left), differently from the stable flame (black curve), no clear resonant peaks are observed.

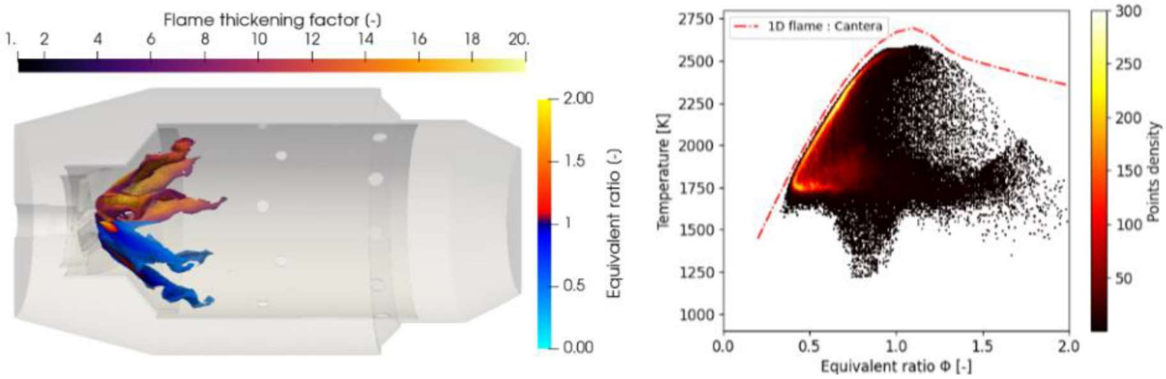

(a) (b)

Figure 3. (a) Heat release rate region coloured by the flame temperature and equivalence ratio (b) scatter plot of temperature over local equivalence ratio.

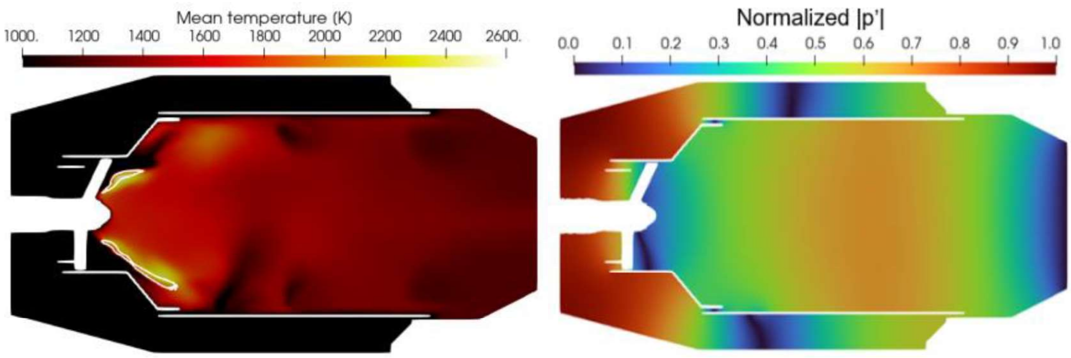

(a) (b)

Figure 4. (a) Time averaged of the temperature field over five flow-through times and the iso-contour of heat release rate (white lines) at 10 % of the highest value. (b) Second acoustic mode evaluated by FEniCS.

On the contrary, some unstable modes are triggered (red curve) at a frequency of ~ 900 Hz and 2200 Hz when a relaxation factor of $60 \cdot 10^3\ s^{-1}$ is applied at both inlet and outlet. These correspond to the first and second acoustic modes, respectively, evaluated by FEniCS (Fig. 4b). The peaks are recorded also in the heat release rate spectrum confirming the thermoacoustic coupling (Fig. 5a-right). A trace of the two modes can be also found in the pressure spectrum of sound recorded during the mGT tests with an external microphone (Fig. 5b), indicated with blue and red line, which validates the LES predictions.

Conclusions

Reactive fully compressible LES simulations have been performed on the MTT Enertwin mGT combustor. The results showed a stable V-shape flame without any acoustic mode except when the relaxation factor at inlet and outlet are changed. Frequency peaks are excited at approx. 900 and 2200 Hz which are close to those coming from the experimental data, proving the reliability of the applied procedure.

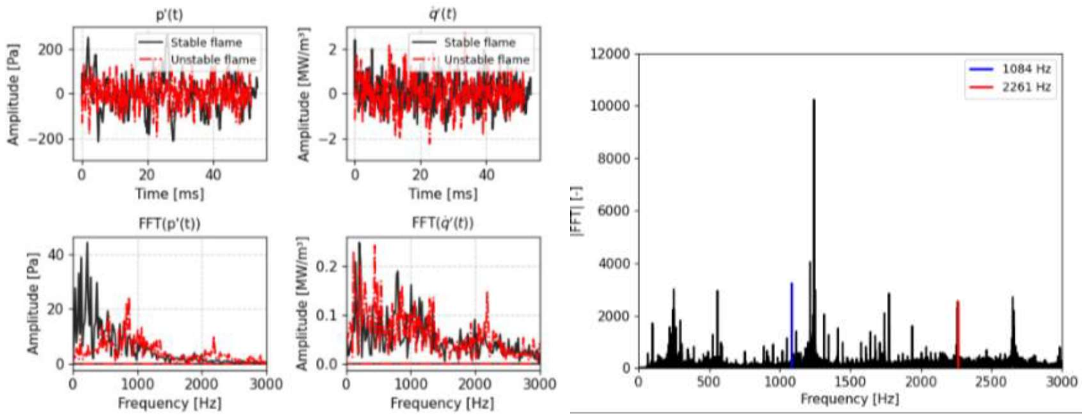

(a) (b)

Figure 5. (a) FFT analysis of the pressure and heat release rate signals where black and red are the stable and unstable flame respectively. (b) FFT analysis of the sound emitted by the mGT while operating at nominal condition.

Acknowledgments

HPC resources from EuroHPC JU (Project PROMETH2EUS) on MeluXina/LuxProvide and from CRESCO/ENEAGRID are acknowledged.

References

[1] Agostinelli, P. W., Laera, D., Boxx, I., Gicquel, L., & Poinsot, T. (2021). Impact of wall heat transfer in Large Eddy Simulation of flame dynamics in a swirled combustion chamber. *Combustion and Flame* 234, 111728.

[2] Gicquel, L. Y., Staffelbach, G., & Poinsot, T. (2012). Large eddy simulations of gaseous flames in gas turbine combustion chambers. *Progress in energy and combustion science* 38(6), 782-817.

[3] Poinsot, T.J., Lelef, S.K., Boundary conditions for direct simulations of compressible viscous flows, *Computational Physics* 101(1):104-129 (1992)

[4] Legier, J.P., Poinsot, T., Veynante, D., *Dynamically thickened flame LES model for premixed and non-premixed turbulent combustion*, Proceedings of the summer program, 2000, p. 157-168.

[5] Charlette, F., Meneveau, C., Veynante, D., "A power-law flame wrinkling model for LES of premixed turbulent combustion Part I: non-dynamic formulation and initial tests", *Combustion and Flame* 131:159-180 (2002)

[6] Charlette, F., Meneveau, C., Veynante, D., "A power-law flame wrinkling model for LES of premixed turbulent combustion Part II: dynamic formulation", *Combustion and Flame* 131:181-197 (2002)

[7] De Santis, A., Clements, A.G., Pranzitelli, A., Ingham, D.B., Pourkashanian, M., "Assessment of the impact of subgrid-scale stress models and mesh resolution on the LES of a partially-premixed swirling flame", *Fuel* 281: 118620 (2020)

[8] Franzelli, B., Riber, E., Gicquel, L., Poinsot, T., "Large eddy simulation of combustion instabilities in a lean partially premixed swirled flame", *Combustion and Flame* 159:621-637 (2012)

[9] Selle, L., Nicoud, F., Poinsot, T., "Actual impedance of nonreflecting boundary conditions: Implications for computation of resonators", *AIAA* 42: 958-964 (2004)